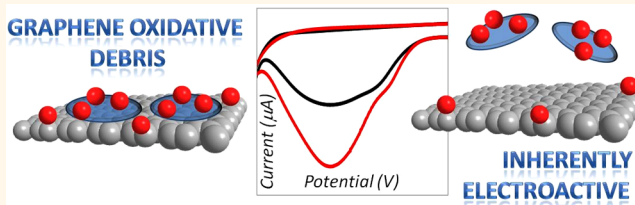


Oxidation Debris in Graphene Oxide Is Responsible for Its Inherent Electroactivity

Alessandra Bonanni, Adriano Ambrosi, Chun Kiang Chua, and Martin Pumera*

Division of Chemistry & Biological Chemistry, School of Physical and Mathematical Sciences, Nanyang Technological University, Singapore 637371

ABSTRACT



Graphene oxide is known to exhibit many interesting properties, ranging from inherent fluorescence to inherent electrochemistry, just to name a few. Recent research has found that graphene oxide is a composite material consisting of the so-called “oxidation debris” and unoxidized graphene fragments. Surprisingly, the oxidation debris, which contains small and highly oxidized aromatic fragments adsorbed on graphene surfaces, is responsible for the excellent solubility and inherent fluorescence of graphene oxide. Here, we examine the origin of the inherent electroactivity of graphene oxide and demonstrate that such phenomenon is attributed to the presence of oxidation debris. We separate oxidation debris from the less oxidized graphene backbone in “as-prepared” graphene oxide nanoplatelets using ultrasonication. We found that the extension of ultrasonication time corresponded to a larger amount of oxidation debris released from the graphene oxide nanoplatelets’ surfaces and subsequently caused detrimental effects to the inherent electroactivity of the graphene material. Since graphene oxide is often the material of choice for energy storage devices, such as batteries and supercapacitors, a thorough understanding on the origin of such inherent electrochemical properties of graphene oxide is of very high importance.

KEYWORDS: oxidation debris · graphene oxide · inherent electroactivity

Graphene oxide, a well-celebrated graphene-based material, exhibits many interesting properties, stretching from its excellent solubility in aqueous solutions¹ to its inherent fluorescence² or inherent electrochemistry.³ These properties are exploited in many applications, *e.g.*, in sensing and biosensing^{4,5} or energy storage devices.^{6–8} Surprisingly, the exact chemical structure of graphene oxide (GO) remains unclear up to now.⁹ It is only recently that graphene oxide has been shown to be a highly heterogeneous material that consists of poorly oxidized graphene sheets and highly oxidized graphene debris.¹ This oxidation debris is often responsible for the observed excellent solubility in aqueous solutions¹ or fluorescence² of graphene oxide. Oxidation debris (OD) can be defined as highly oxidized polyaromatic fragments

strongly adsorbed on the graphene matrix by π – π stacking, hydrogen bonding, and van der Waals interactions.^{1,10} Oxidation debris (sometimes also referred to as carboxylated carbonaceous fragments¹¹) has been investigated previously as a product of nitric acid purification treatment of carbon fibers and carbon nanotubes (CNT).^{11–17} It was discovered that the amount of carbonaceous debris strongly depended on the time length of the oxidation treatment of carbon fibers, ranging from 0.11 to 22.1% (wt).¹² The oxidation debris was found to strongly influence spectroscopic properties of single-walled carbon nanotubes¹³ as well as its fluorescence.¹⁴ In addition, the presence of oxidation debris altered the solubility of CNTs¹⁵ and was also found to be partly responsible for the toxicity of CNTs.¹⁶ It was further shown that oxidation debris on

* Address correspondence to pumera@ntu.edu.sg.

Received for review August 14, 2013 and accepted April 26, 2014.

Published online April 30, 2014
10.1021/nn404255q

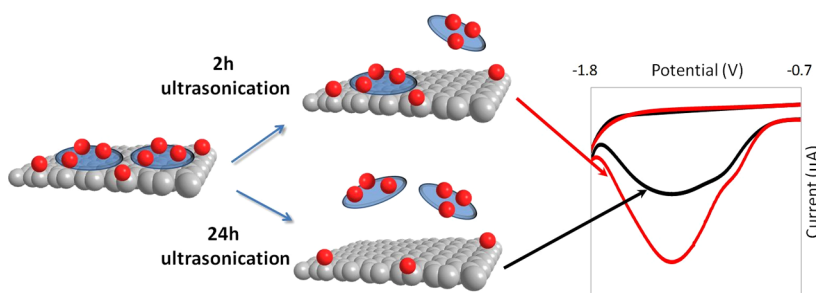
© 2014 American Chemical Society

carbon nanotubes presents significant problems for subsequent covalent functionalization, owing to the fact that most of the reactive carboxylic groups were present on the oxidation debris, which was noncovalently bound to CNTs.^{11,17} Even though the presence of oxidation debris was clearly identified, its exact nature remained elusive. Specifically, its size and chemical composition were not conclusively determined. Oxidation debris was previously suggested to be benzopolycarboxylic acid,¹⁸ while other works suggested the size of 10–15 polyaromatic molecule containing various oxygen-containing groups, ranging from carboxyl to epoxide and hydroxyl¹² with molecular weight of 200–800 Da,¹⁶ possibly with a structure similar to fulvic acid;¹⁴ however, the suggestion on structure similarity to fulvic acid was challenged,¹⁶ and larger structures of oxidation debris, up to 5 nm, were suggested instead.^{15,19} Analogous to previous findings for carbon nanotubes,^{11–17,19} recent works have also demonstrated the presence of oxidation debris on graphene materials.^{1,2,10,20,21} Several chemical and physical properties, which were previously attributed to the “as-prepared” graphene oxide itself, are now being re-examined in order to fully understand the influence and role of such oxidation debris. Recently, in an elegant work from Rourke’s group, OD was successfully separated from GO by using a base-washing protocol and was estimated to make up for one-third of the whole GO mass.¹ A further study by the same group was performed to identify the role of OD on graphene oxide fluorescence.² In a separate study, an enhanced catalytic activity on the oxidative coupling of amines to imines was achieved with porous graphene which had its OD removed by base-washing treatment.²⁰ The variable surface properties of GO with and without OD were also assessed by anchoring Ag nanoparticles on the oxygen-containing groups of GO.¹⁰ Under similar circumstances as previous research on the oxidation debris of CNTs, the exact structure of oxidation debris on the surface of graphene remains elusive. On the basis of X-ray photoelectron spectroscopy data, it was suggested that the oxidation debris contained carboxyl, epoxide, and hydroxyl groups.²² It was also found that the size of the oxidation debris was ~1 nm or less, which was effectively the size of 3–4 aromatic rings.²³ It should be mentioned that reduced graphene contains small organic aromatic molecules which desorb at temperatures as low as 50 °C.²⁴ The electrochemical behaviors of GO and reduced GO, either debris-free or containing oxidation debris, were studied with various redox probes to demonstrate the detrimental effects of OD on the heterogeneous electron transfer properties of the graphene materials.²¹ The different chemical and physical properties observed in debris-free GO were mainly due to the reduced presence of oxygen functionalities on GO surfaces. In fact, a drastic increase in C/O atomic ratio has been observed on

debris-free GO,^{1,10} which indicated that the oxygen functionalities on “as-prepared” GO were mainly concentrated on the OD surfaces. The electrochemistry of graphene oxide described above refers to the oxidation/reduction of solutes (based on *heterogeneous electron transfer* phenomenon). In addition, there exists another aspect of electrochemistry which is highly of interest to us in this work, whereby GO shows *inherent* electrochemistry, that is, it contains oxygen-containing groups (*i.e.* epoxide, aldehyde, or peroxide) which can be electrochemically reduced at mild potentials.³

Given the widespread application of graphene oxide in energy storage devices,⁸ solar cells^{25,26} and biosensing,²⁷ the frequently observed *inherent* electrochemical activity (as opposed to *heterogeneous electron transfer*, the *inherent* electrochemistry refers to the *inherent* reduction of the material itself) of graphene oxide thus begs the question: is the oxidation debris then involved in the *inherent* electroactivity of GO? It is well-established that the reduction peaks observed in GO materials at cathodic potentials are due to the presence of oxygen-containing groups such as epoxides, peroxides, and aldehydes on their surfaces.^{3,28} As such, the electrochemical reduction of GO has been exploited by several groups to either obtain reduced graphene platforms with specific characteristics and functionalities^{3,29} or as a working signal whereby GO is used as a label for biosensing.^{27,30} Due to the considerable number of applications, it is therefore important to obtain deeper insights into the origin of the electrochemical signal provided by GO reduction. Note that the *inherent* electrochemistry of graphene oxide itself is a conceptually different phenomenon from the *heterogeneous electron transfer* electrocatalysis of graphene toward solutes (peroxides, glutathione, etc.) in which the latter was reported to be caused by metallic impurities within the graphene materials.^{31,32}

In this work, we are interested in investigating the *inherent* electroactivity of GO in order to understand the role of oxidation debris on this property. Analogous to the usage of ultrasonication for the exfoliation of graphite oxide to graphene oxide,³³ we developed a protocol based on the prolonged ultrasonication of GO to achieve the separation of oxidation debris from the graphene matrix. The electrochemical signals due to the ‘as-prepared’ GO, debris-free GO, and oxidation debris were measured and compared among different ultrasonication times. UV–visible spectroscopy, Fourier transform infrared spectroscopy (FTIR), X-ray photoelectron spectroscopy (XPS), elemental analysis (EA), scanning transmission electron microscopy (STEM), Raman spectroscopy, and inductively coupled plasma mass spectrometry (ICP-MS) investigations were also performed to confirm and support the results obtained by electrochemistry.



Scheme 1. Schematic of the experimental protocol.

RESULTS AND DISCUSSION

To address the question on whether the oxidation debris is responsible for the *inherent* electroactivity of graphene oxide, the oxidation debris was thus separated from graphene sheets using ultrasonication.^{11,19,34} The electrochemical behaviors of graphene oxide nanoplatelets (GONPs) subjected to different extent of ultrasonication times were studied. Scheme 1 illustrates the experimental procedure in which different amount of oxidation debris is removed from GONPs after different ultrasonication times and how such time variable influences the inherent electroactivity of GONPs.

In our initial approach to the investigation, four solutions of graphite oxide nanofibers (GONFs) were prepared and ultrasonicated with increasing times of 2, 8, 16, and 24 h in order to obtain the respective graphene oxide nanoplatelets solutions: aGONP-2h, aGONP-8h, aGONP-16h, and aGONP-24h (where 'a' stands for "as-prepared"). Figure 1 illustrates the cyclic voltammograms obtained from the electrochemical reduction of the four GONPs which were drop-casted onto glassy carbon (GC) electrode surfaces. The observed voltammetric peaks around -1.4 V originated from the *inherent* electroactivity of GONPs and correlated to the presence and amount of oxygen functionalities on the graphene surfaces.^{28,35} As it can be seen in Figure 1, the intensity of the reduction peaks decreased when the ultrasonication time was extended from 2 to 24 h. Given the fact that most of the oxygen-containing groups are concentrated on the OD surfaces,^{1,2,10,21} the decrement in the *inherent* electroactivity of graphene oxide can thus be attributed to a reduced amount of oxygen functionalities on GONP surfaces as a consequence of OD removal due to prolonged ultrasonication time.

To gain deeper insights into the role of OD on the inherent electroactivity of GONPs, the aGONPs were separated by centrifugation¹ into two different portions: (i) a supernatant solution containing the oxidation debris (OD) and (ii) a debris-free GONP precipitate (pGONP). For this study, we chose to focus only on the two extreme cases, specifically the aGONP-2h and aGONP-24h.

Figure 2 illustrates the electrochemical behaviors of aGONP-2h and aGONP-24h before (panel a) and after

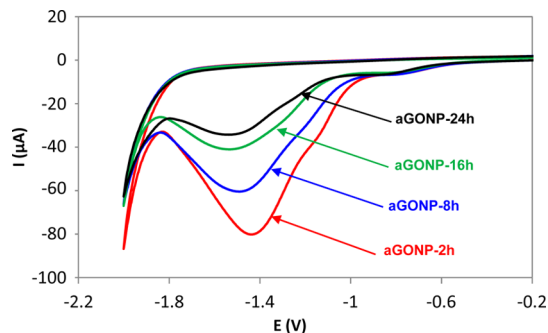


Figure 1. Cyclic voltammetry (CV) of "as-prepared" GONPs (aGONPs) after ultrasonication times of 2 h (red line), 8 h (blue line), 16 h (green line), and 24 h (black line). All measurements were performed in 0.1 M PBS, pH 7.

the respective ODs have been separated from aGONPs (panels b and c). As shown in Figure 2b for GONP treated with 2 h of ultrasonication, the largest peak was observed for the starting material aGONP-2h and followed by pGONP-2h. The peak with the lowest intensity was provided by the supernatant solution containing the oxidation debris, OD-2h. These results showed that pGONP-2h was responsible for most of the electroactivity of aGONP-2h while only a small fraction of it was due to OD-2h. It was also apparent from the subsequent structural and morphological characterizations (see below) that only a partial removal of OD from aGONP surface was achieved after 2 h of ultrasonication treatment meaning that most of the OD was still adsorbed on the pGONP surface.

As for GONP treated with 24 h of ultrasonication, OD-24h was responsible for most of the electroactivity of aGONP-24h, while the pGONP-24h showed a much reduced electroactivity. In this case, a significant desorption of OD from aGONP surface has occurred after 24 h of ultrasonication, as confirmed by the increased reduction signal of OD in the supernatant. The clear differences in the electrochemical behaviors of OD-2h and OD-24h relative to their respective pGONPs established the fact that most of the OD was still retained on the graphene materials even after 2 h of ultrasonication, while a 24 h ultrasonication treatment was able to desorb most of the OD.

These findings were supported by FTIR analyses (Figure S1, Supporting Information). FTIR data showed

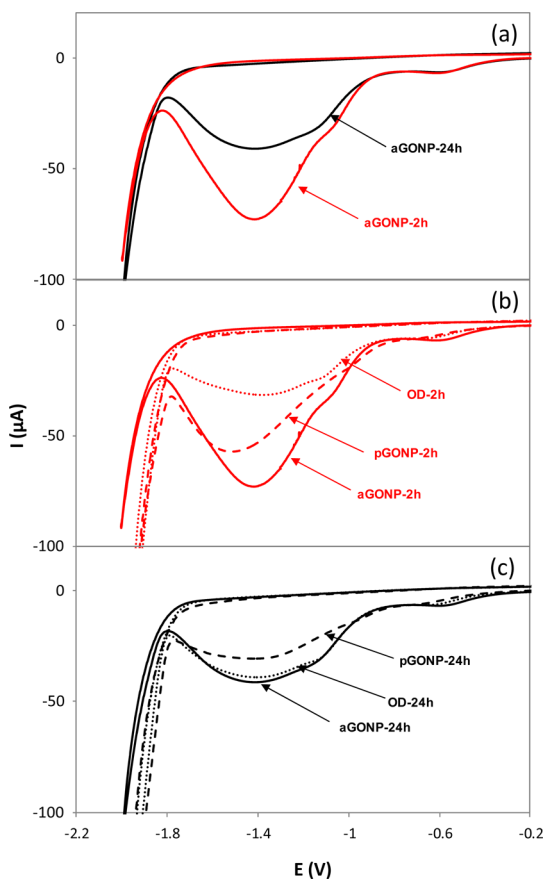


Figure 2. Cyclic voltammetry (CV) of “as-prepared” GONPs (aGONPs), precipitated GONPs after centrifugation (pGONPs), and supernatant containing oxidation debris (OD). (a) CV for “as-prepared” GONPs after 2 h (aGONP-2h) and 24 h (aGONP-24h) of ultrasonication; (b) CV for “as-prepared” GONPs after 2 h of ultrasonication (aGONP-2h), precipitated GONPs (pGONP-2h) and oxidation debris (OD-2h) obtained after centrifugation of aGONP-2h; (c) CV for “as-prepared” GONPs after 24 h of ultrasonication (aGONP-24h), precipitated GONPs (pGONP-24h) and oxidation debris (OD-24h) obtained after centrifugation of aGONP-24h.

C=C band at 1603 cm^{-1} and C=O band at 1714 cm^{-1} . It can be seen that there was a quantitative increase in the ratio of C=C band to C=O band on pGONP after the removal of oxidation debris (even after 2 h of ultrasonication), which indicated that there was less oxygen-containing groups present on the pGONP than on GONP. This is consistent with previous FTIR observations on graphene oxide before and after removal of oxidation debris.¹⁰ The band at $2700\text{--}3000\text{ cm}^{-1}$ is related to C-H stretch.³⁶ While the intensity of this band was low on GONP and pGONP-2h, it was prominent on pGONP-24h. The presence of C-H stretch was also observed previously on graphene oxide and oxidation debris-free graphene oxide, with intensities similar to that observed here on GONP and pGONP-2h.¹⁰ The intensity of the C-H band was stronger on pGONP-24h than pGONP-2h, which can be explained either by the fact that a longer ultrasonication time has led to a more effective removal of OD or structural rearrangement of graphene oxide.³⁷

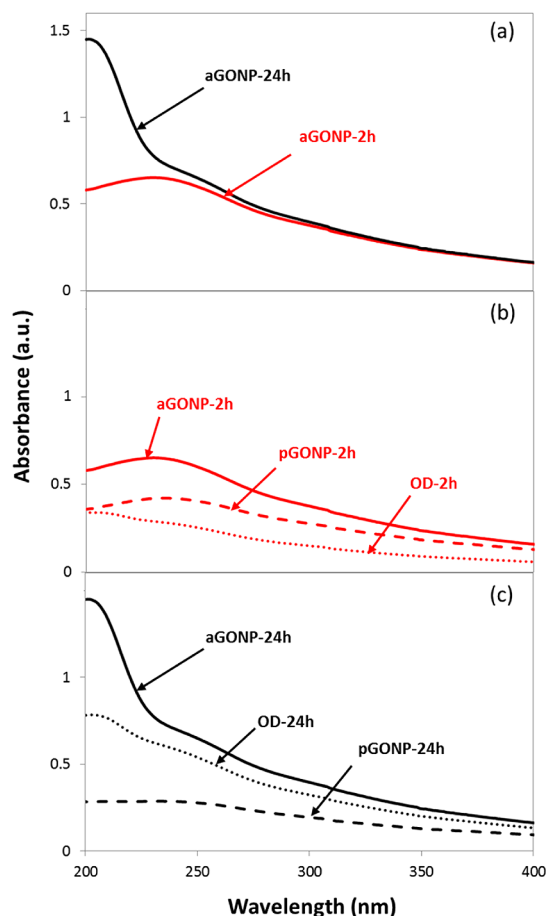


Figure 3. UV-vis absorption spectra of “as-prepared” GONPs (aGONPs), precipitated GONPs after centrifugation (pGONPs), and supernatant containing oxidation debris (OD). (a) UV-vis spectra for “as-prepared” GO NPs after 2 h (aGONP-2h) and 24 h (aGONP-24h) of ultrasonication; (b) UV-vis spectra for “as-prepared” GONPs after 2 h of ultrasonication (aGONP-2h), precipitated GONPs (pGONP-2h) and oxidation debris (OD-2h) obtained after centrifugation of aGONP-2h; (c) UV-vis spectra for “as-prepared” GONPs after 24 h of ultrasonication (aGONP-24h), precipitated GONPs (pGONP-24h) and oxidation debris (OD-24h) obtained after centrifugation of aGONP-24h.

To further justify our findings, the graphene materials were analyzed by UV-vis spectroscopy. Figure 3 illustrates UV-vis spectra of aGONP-2h and aGONP-24h before (panel a) and after the separation of OD from the respective aGONPs (panels b and c). As shown in Figure 3a, aGONP-2h gave a typical GO absorbance peak around 230 nm ,^{29,38} while aGONP-24h showed a larger absorbance peak shifted toward the lower wavelength region. The blue-shifted and larger peak recorded for aGONP-24h was due to the presence of a larger amount of OD released from aGONP surface into the aqueous solution after 24 h of ultrasonication. This observation was also supported by previous studies in which a higher oxidation degree of graphene material corresponded to blue-shifted absorption peaks.^{39,40}

Once the aGONP solutions were separated into their respective pGONPs and ODs, a different picture was

observed on GONP-2h and GONP-24h. As illustrated in Figure 3b, a larger absorption peak was provided by the debris-free pGONP-2h while a lower absorption peak was observed for the supernatant containing OD. This meant that, in reference to the electrochemical results above, most of the OD was still retained by pGONP-2h while only a small fraction was present in the separated supernatant. When the ultrasonication time was increased from 2 to 24 h, the absorption signal due to the separated OD increased dramatically while the pGONP-24h showed very low absorption intensity, thus confirming the massive desorption of OD from the aGONP surface after 24 h of ultrasonication treatment. In addition to the UV-vis measurements, physical difference between the aGONPs suspensions was also striking even on plain sight (Figure S2, Supporting Information). Whereas the aGONP-2h showed a typical brownish color of graphene oxide solution,³³ aGONP-24h showed a darker color which distinctively reflected the presence of debris-free graphene sheets.^{1,10}

XPS analysis was subsequently performed to investigate the amount of oxygen-containing groups on GONP surfaces after the ultrasonication treatments. Figure 4 illustrates the C 1s core level spectra for untreated graphite nanofibers (panel A) and debris-free precipitates obtained after the centrifugation of aGONPs that were ultrasonicated for 2 h (panel B) and 24 h (panel C). The results obtained from the XPS analysis were consistent with previous reports.^{1,10} As seen in Figure 4A, the peak centered at 284.5 eV corresponded to C=C sp² bonds, while the higher binding energy components were due to oxygen functionalities present on GONF surface. A lower amount of oxygen functionalities (Figure 4B) was found on the precipitate from after 2 h of ultrasonication treatment (pGONP-2h), as compared to the starting material. Moreover, a further reduction was observed (Figure 4C) upon a longer period of ultrasonication treatment (pGONP-24h) (for the deconvolution of XPS analysis, please refer to Figure S5). The C 1s core level spectrum of the untreated starting material, GONFs, can be deconvoluted with three peaks at binding energies of 284.5 (56%), 286.7 (34%), and 288.7 eV (10%) which can be assigned to C=C sp² bonds, C—O bonding, and C=O bonding, respectively. The C 1s core level spectrum of the residual material after 2 h of ultrasonication, pGONPs-2h, was also deconvoluted with three peaks at 284.5 (60%), 286.4 (33%), and 288.6 eV (7%). It can be noted that the oxygen functionalities decreased from a total peak area of 44% to about 40%. On the other hand, the C 1s core level spectrum for the residual material after 24 h of ultrasonication, pGONPs-24h, was deconvoluted with four peaks centered at 284.5 (62%), 286.3 (27%), 288.3 (8%), and 290.4 eV (3%). In addition to the C=C, C—O, and C=O bonding, the peak at 290.4 eV can be assigned to O—C=O group. The total count of oxygen functionalities for pGONPs-24h was about 38%.

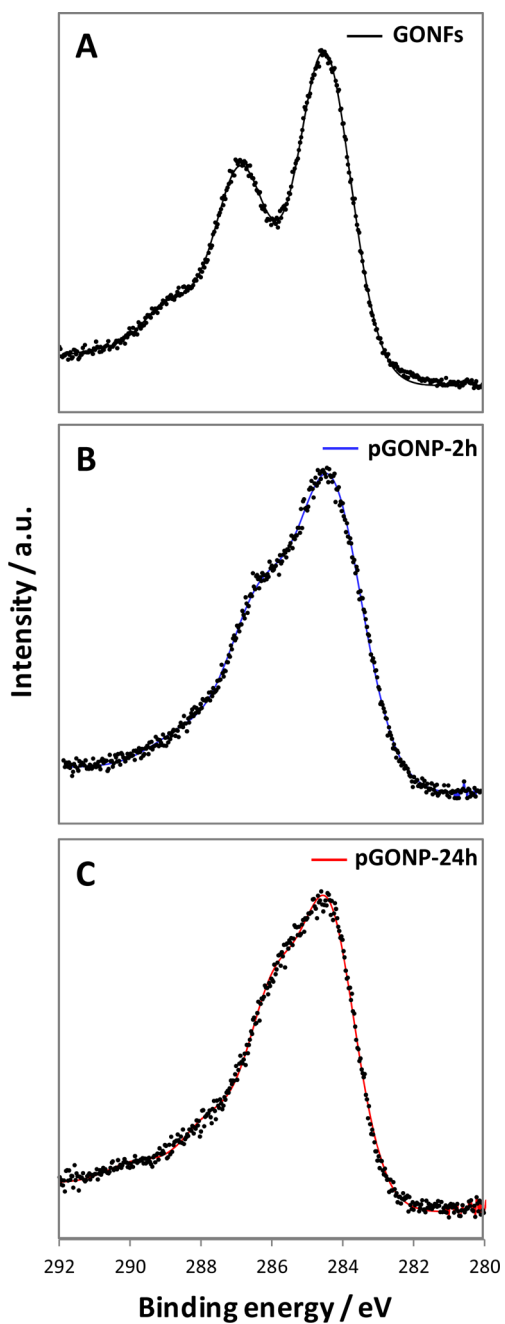


Figure 4. High-resolution XPS C 1s core level spectra of GONFs and GONPs. (A) Untreated graphite oxide nanofibers (GONFs); (B) debris-free precipitate obtained from graphene oxide nanplatelets ultrasonicated for 2 h (pGONP-2h); (C) debris-free precipitate obtained from graphene oxide nanplatelets ultrasonicated for 24 h (pGONP-24h).

A further decrease, albeit little, of oxygen functionalities was registered after a longer ultrasonication time. Since carboxylic groups are generally present at the edges of graphene materials,⁴¹ the longer ultrasonication time which caused more damages to the material could have most likely favored the formation of oxygen functionalities at the edges. This substantiated our previous findings that a prolonged ultrasonication treatment can effectively remove the oxidation debris, where bulk of

the oxygen-containing groups reside on, from the GONP surfaces. Further evidence to our hypothesis was provided by elemental analysis performed on debris-free precipitate obtained from GONP ultrasonicated for 24 h (pGONP-24h). The C/O ratio found for pGONP-24h was 2.55 (%C, 42.06; %O, 16.70; %H, 41.23; %N, 0; %S, 0), which was much higher than the starting material, GONFs, at 1.44 (%C, 42.33; %O, 29.24; %H, 28.43; %N, 0; %S, 0).

To further investigate the effects of ultrasonication time on the morphological and structural properties of both the "as-prepared" GONP and debris-free GONP, STEM, and Raman spectroscopy were performed on the studied materials. The STEM image of GONFs showed the individual nanofiber structures in which the graphene sheets were aligned perpendicularly along the fiber axis (see Figure S3A, Supporting Information). Upon chemical oxidation and after 2 and 24 h of ultrasonication treatments, separated graphene oxide nanoplatelets were observed (Figure S3B–E). From the figures, it was obvious that the "as-prepared" GONPs treated with 2 h of ultrasonication (aGONP-2h, panel B) and debris-free precipitate (pGONP-2h, panel C) obtained from aGONP-2h showed a similar structure. In addition, the "as-prepared" GONPs obtained after 24 h of ultrasonication treatment (aGONP-24h, panel C) and debris-free precipitate (pGONP-24h, panel D) obtained from aGONP-24h showed a similar structure. This was in agreement with previous works in which it was not possible to distinguish "as-prepared" GO from debris-free GO by using STEM technique.²² Despite that, the STEM analysis was able to provide evidence on the extent of exfoliation of the graphene materials. It was apparent from the STEM images that an ultrasonication treatment of 24 h (panels D and E) was able to provide a more effective exfoliation as compared to just 2 h of ultrasonication treatment (part B and C). It is known that extended ultrasonication treatment of graphitic/graphenic materials leads to the fragmentation of these materials from an original size of several tens of micrometers to micrometer or even submicrometer sizes.^{42–45} This is of course dependent on the applied power of ultrasonication, bath temperature, and

whether any cavitation takes place. Since GONPs utilized in this study have base dimensions of 50 × 50 nm, they are much smaller than micrometer sized graphene sheets studied previously.^{42–45} Moreover, since the size of oxidation debris has been suggested to be <1 nm in previous works,^{11–17,23} it was expected that the "as prepared" and debris-free GO should not show any structural difference. A similar result was previously observed in a different work.²²

Furthermore, Raman spectroscopy is an extremely important tool for the characterization of graphene materials.⁴⁶ Raman spectrum of graphene materials is generally analyzed by evaluating two prominent features: the G-band around 1600 cm^{−1}, which corresponds to sp² lattice, and the D band around 1300 cm^{−1}, which is related to the presence of defects in the sp² lattice. As shown in Figure S4, the variations of D/G ratio for GONFs, aGONP-2h, pGONP-2h, aGONP-24h, pGONP-24h were within the statistical error,⁴⁷ suggesting a structural similarity of all the analyzed graphene materials.

CONCLUSIONS

The inherent electroactivity of graphene oxide nanoplatelets has been investigated, and the role of oxidation debris on this property has been clarified. A prolonged ultrasonication treatment is introduced to separate the native GONPs from the OD fraction. UV–vis studies, FTIR, XPS, EA, STEM, Raman, and ICP-MS investigations were also performed on the graphene materials in support of the electrochemical results. We found that the separation of OD from the "as-prepared" GONPs corresponded to a net reduction in the inherent electroactivity of graphene oxide nanoplatelets. This is because as the ultrasonication time increases, a larger amount of OD is released from the aGONPs. This demonstrates that the electroactivity of graphene oxide mostly resides in the oxidation debris. Moreover, it is clear that different ultrasonication processing times dramatically changes the electrochemical properties of graphene oxides. These finding will have profound impacts on the application of graphene oxide in electrochemical devices, such as batteries, supercapacitors, or sensors.

EXPERIMENTAL SECTION

Materials. Stacked graphite nanofibers were provided by Strem Chemicals (Newburyport, MA). Potassium permanganate, hydrogen peroxide, sulfuric acid (95–98%), and sodium nitrate were obtained from Sigma-Aldrich (Singapore). Phosphate buffer solution used in the study was the following: 0.1 M PBS (0.1 M NaCl and 10 mM sodium phosphate buffer, pH 7.0). All solutions were prepared using Milli-Q water (18.2 MΩ cm resistivity). Glassy carbon electrodes, each with an effective surface area of 7.07 mm², were provided by EcoChemie (The Netherlands). The three-electrode cell includes a glassy carbon working electrode, a platinum counter electrode, and a Ag/AgCl reference electrode.

Equipment. An Autolab PGSTAT302 potentiostat (Eco Chemie, Utrecht, The Netherlands) driven by GPES software, version 4.9 was used to carry out all electrochemical experiments. Cyclic voltammetry (CV) measurements were performed in PBS buffer solution at 0.1 V s^{−1}. UV–vis measurements were performed by using a UV/vis spectrophotometer, dual beam UV-2550 (Shimadzu, Japan). The optical cell thickness for UV–vis measurements was 0.1 cm. An Allegra 64R centrifuge (Beckman Coulter, Singapore) was used for GONPs preparation/separation protocols. Ultrasonication of GONPs was performed in a FB11203 ultrasonicator (Thermo Fisher Scientific, Singapore), at a frequency of 37 kHz. Ultrasonication temperature was controlled using an ice bath and always maintained lower than 30 °C. XPS study was performed with a Phoibos 100 spectrometer and a

Mg X-ray radiation source (SPECS, Germany); Raman spectroscopy was carried out with a confocal micro-Raman LabRam HR instrument from Horiba Scientific in backscattering geometry with a CCD detector, a 514.5 nm Ar laser, and a 100 \times objective mounted on a Olympus optical microscope. Combustible elemental analysis was performed on a EuroVector Euro EA elemental analyzer; ICP-MS was carried out with an Agilent model 7700 \times ICP-MS, while microwave digestion in concentrated nitric acid was carried out in a Mars CEM system. The obtained results for the element concentrations were the following: 8.18, 0.14, 29.62, 20.10, and 5248.71 ppm for Fe, Co, Mo, Ni, and Mn, respectively. The levels of Cu and Zn were found to be lower than those of the detection limit.

A JEOL JSM-7600F semi-in-lens FE-SEM was used to acquire the STEM images. Attenuated total reflectance Fourier transform infrared (ATR-FTIR) characterization was performed using a PerkinElmer Spectrum 100 system coupled with a universal ATR accessory. A diamond/ZnSe was employed as the ATR crystal.

Procedures. Conventional protocols were followed to prepare bulk quantities of graphene oxide nanoplatelets.³⁸ Graphite oxide nanoplatelets were prepared from graphite nanofibers by following a modified Hummers' method.^{48,49} A total of 0.5 g of graphene nanofibers was mixed together with 0.5 g of NaNO₃ and 23 mL of H₂SO₄, and the mixture was stirred in an ice bath. Subsequently, 3 g of KMnO₄ was slowly added to the mixture while the temperature was maintained at 0 °C. The solution was then heated to 35 °C and stirred for 1 h. After the formation of a thick paste, 40 mL of water was added, and the solution was stirred for an additional 30 min at 90 °C. Subsequently, 100 mL of water was added into the mixture followed by 3 mL of H₂O₂ (30%) until the evolution of gas ceased. The mixture was then filtered and washed with 100 mL of warm water. This was followed by a redispersion of the filtered material in water. The solution was then centrifuged at 8000 rpm for 15 min and washed with water until the supernatant reached a neutral pH. The obtained GONFs powder was last dried in an oven for 2 days at 60 °C.

A 1 mg mL⁻¹ water solution of obtained graphite oxide nanofiber (GONF) powder was ultrasonicated for 2 h in order to obtain graphene oxide nanoplatelets (GONPs).³³ Ultrasonication of 1 mg mL⁻¹ of GONFs suspension for the different experiments was performed for 2, 8, 16, and 24 h under a controlled temperature of 25 °C.⁴² For electrochemical measurements, 1 μ L of a GONP 1 mg mL⁻¹ suspension in Milli-Q water was drop-casted on a glassy carbon electrode surface and allowed to dry at room temperature. For UV-vis experiments, a 0.02 mg mL⁻¹ suspension was employed. For the separation of oxidation debris, the GONP suspensions ultrasonicated for different times were centrifuged at 15 000 rpm for 1 h. After that, the supernatants were collected and the precipitates were washed with Milli-Q water for 3 times and resuspended in the same volume of water. The solution mixture was then transferred into a Petri dish and left in an oven at 40 °C for 2 days. A 1 mg mL⁻¹ suspension in Milli-Q water was prepared with the obtained graphene powder. The ratios of pGONP/OD upon 2 and 24 h of ultrasonication treatments were found to be 70:30 and 46:54, respectively.

Conflict of Interest: The authors declare no competing financial interest.

Supporting Information Available: FTIR, STEM, XPS and Raman characterizations. This material is available free of charge via the Internet at <http://pubs.acs.org>.

REFERENCES AND NOTES

- Rourke, J. P.; Pandey, P. A.; Moore, J. J.; Bates, M.; Kinloch, I. A.; Young, R. J.; Wilson, N. R. The Real Graphene Oxide Revealed: Stripping the Oxidative Debris from the Graphene-like Sheets. *Angew. Chem., Int. Ed.* **2011**, *50*, 3173–3177.
- Thomas, H. R.; Valles, C.; Young, R. J.; Kinloch, I. A.; Wilson, N. R.; Rourke, J. P. Identifying the Fluorescence of Graphene Oxide. *J. Mater. Chem. C* **2013**, *1*, 338–342.
- Zhou, M.; Wang, Y. L.; Zhai, Y. M.; Zhai, J. F.; Ren, W.; Wang, F. A.; Dong, S. J. Controlled Synthesis of Large-Area and Patterned Electrochemically Reduced Graphene Oxide Films. *Chem.—Eur. J.* **2009**, *15*, 6116–6120.
- Liu, F.; Choi, J. Y.; Seo, T. S. Graphene Oxide Arrays for Detecting Specific DNA Hybridization by Fluorescence Resonance Energy Transfer. *Biosens. Bioelectron.* **2010**, *25*, 2361–2365.
- Wu, X.; Tian, F.; Wang, W.; Chen, J.; Wu, M.; Zhao, J. X. Fabrication of Highly Fluorescent Graphene Quantum Dots Using L-Glutamic Acid for *in Vitro/in Vivo* Imaging and Sensing. *J. Mater. Chem. C* **2013**, *1*, 4676–4684.
- Hsieh, C. T.; Teng, H. Influence of Oxygen Treatment on Electric Double-Layer Capacitance of Activated Carbon Fabrics. *Carbon* **2002**, *40*, 667–674.
- Bao, Q. L.; Bao, S. J.; Li, C. M.; Qi, X.; Pan, C. X.; Zang, J. F.; Lu, Z. S.; Li, Y. B.; Tang, D. Y.; Zhang, S.; et al. Supercapacitance of Solid Carbon Nanofibers Made from Ethanol Flames. *J. Phys. Chem. C* **2008**, *112*, 3612–3618.
- Xu, B.; Yue, S. F.; Sui, Z. Y.; Zhang, X. T.; Hou, S. S.; Cao, G. P.; Yang, Y. S. What Is the Choice for Supercapacitors: Graphene or Graphene Oxide? *Energy Environ. Sci.* **2011**, *4*, 2826–2830.
- Szabo, T.; Berkesi, O.; Forgo, P.; Josepovits, K.; Sanakis, Y.; Petridis, D.; Dekany, I. Evolution of Surface Functional Groups in a Series of Progressively Oxidized Graphite Oxides. *Chem. Mater.* **2006**, *18*, 2740–2749.
- Faria, A. F.; Martinez, D. S. T.; Moraes, A. C. M.; da Costa, M.; Barros, E. B.; Souza, A. G.; Paula, A. J.; Alves, O. L. Unveiling the Role of Oxidation Debris on the Surface Chemistry of Graphene through the Anchoring of Ag Nanoparticles. *Chem. Mater.* **2012**, *24*, 4080–4087.
- Salzmann, C. G.; Llewellyn, S. A.; Tobias, G.; Ward, M. A. H.; Huh, Y.; Green, M. L. H. The Role of Carboxylated Carbonaceous Fragments in the Functionalization and Spectroscopy of a Single-Walled Carbon-Nanotube Material. *Adv. Mater.* **2007**, *19*, 883–887.
- Wu, Z. H.; Pittman, C. U.; Gardner, S. D. Nitric-Acid Oxidation of Carbon-Fibers and the Effects of Subsequent Treatment in Refluxing Aqueous NaOH. *Carbon* **1995**, *33*, 597–605.
- Hu, H.; Zhao, B.; Itkis, M. E.; Haddon, R. C. Nitric Acid Purification of Single-Walled Carbon Nanotubes. *J. Phys. Chem. B* **2003**, *107*, 13838–13842.
- Wang, Z. W.; Shirley, M. D.; Meikle, S. T.; Whitby, R. L. D.; Mikhalovsky, S. V. The Surface Acidity of Acid Oxidised Multi-Walled Carbon Nanotubes and the Influence of *in Situ* Generated Fulvic Acids on Their Stability in Aqueous Dispersions. *Carbon* **2009**, *47*, 73–79.
- Heister, E.; Lamprecht, C.; Neves, V.; Tilmaci, C.; Datas, L.; Flahaut, E.; Soula, B.; Hinterdorfer, P.; Coley, H. M.; Silva, S. R. P.; et al. Higher Dispersion Efficacy of Functionalized Carbon Nanotubes in Chemical and Biological Environments. *ACS Nano* **2010**, *4*, 2615–2626.
- Stefani, D.; Paula, A. J.; Vaz, B. G.; Silva, R. A.; Andrade, N. F.; Justo, G. Z.; Ferreira, C. V.; Souza, A. G.; Eberlin, M. N.; Alves, O. L. Structural and Proactive Safety Aspects of Oxidation Debris from Multiwalled Carbon Nanotubes. *J. Hazard. Mater.* **2011**, *189*, 391–396.
- Fogden, S.; Verdejo, R.; Cottam, B.; Shaffer, M. Purification of Single Walled Carbon Nanotubes: The Problem with Oxidation Debris. *Chem. Phys. Lett.* **2008**, *460*, 162–167.
- Worsley, K. A.; Kondrat, R. W.; Pal, S. K.; Kalinina, I.; Haddon, R. C. Isolation and Identification of Low Molecular Weight Carboxylated Carbons Derived from the Nitric Acid Treatment of Single-Walled Carbon Nanotubes. *Carbon* **2011**, *49*, 4982–4986.
- Verdejo, R.; Lamoriniere, S.; Cottam, B.; Bismarck, A.; Shaffer, M. Removal of Oxidation Debris from Multi-Walled Carbon Nanotubes. *Chem. Commun.* **2007**, 513–515.
- Su, C. L.; Acik, M.; Takai, K.; Lu, J.; Hao, S. J.; Zheng, Y.; Wu, P. P.; Bao, Q. L.; Enoki, T.; Chabal, Y. J.; et al., Probing the Catalytic Activity of Porous Graphene Oxide and the Origin of This Behaviour. *Nat. Commun.* **2012**, *3*, No. 1298.
- Li, X. M.; Yang, X. Y.; Jia, L.; Ma, X.; Zhu, L. D. Carbonaceous Debris That Resided in Graphene Oxide/Reduced Graphene Oxide Profoundly Affect Their Electrochemical Behaviors. *Electrochem. Commun.* **2012**, *23*, 94–97.

22. Thomas, H. R.; Day, S. P.; Woodruff, W. E.; Vallés, C.; Young, R. J.; Kinloch, I. A.; Morley, G. W.; Hanna, J. V.; Wilson, N. R.; Rourke, J. P. Deoxygenation of Graphene Oxide: Reduction or Cleaning? *Chem. Mater.* **2013**, *25*, 3580–3588.
23. Coluci, V. R.; Martinez, D. S. f. T.; Honório, J. G.; F. de Faria, A. i.; Morales, D. A.; Skaf, M. S.; Alves, O. L.; Umbuzeiro, G. A. Noncovalent Interaction with Graphene Oxide: The Crucial Role of Oxidative Debris. *J. Phys. Chem. C* **2014**, *118*, 2187–2193.
24. Ambrosi, A.; Wong, G. K. S.; Webster, R. D.; Sofer, Z.; Pumera, M. Carcinogenic Organic Residual Compounds Read-sorbed on Thermally Reduced Graphene Materials Are Released at Low Temperature. *Chem. - Eur. J.* **2013**, *19*, 14446–14450.
25. Kavan, L.; Yum, J.-H.; Grätzel, M. Graphene Nanoplatelets Outperforming Platinum as the Electrocatalyst in Co-Bipyridine-Mediated Dye-Sensitized Solar Cells. *Nano Lett.* **2011**, *11*, 5501–5506.
26. Kavan, L.; Yum, J.-H.; Grätzel, M. Optically Transparent Cathode for Co(III/II) Mediated Dye-Sensitized Solar Cells Based on Graphene Oxide. *ACS Appl. Mater. Interfaces* **2012**, *4*, 6999–7006.
27. Loo, A.; Bonanni, A.; Pumera, M. Thrombin Aptasensing with Inherently Electroactive Graphene Oxide Nanoplatelets as Labels. *Nanoscale* **2013**, *5*, 4758–4762.
28. Chng, E. L. K.; Pumera, M. Solid-State Electrochemistry of Graphene Oxides: Absolute Quantification of Reducible Groups Using Voltammetry. *Chem.—Asian J.* **2011**, *6*, 2899–2901.
29. Kotov, N. A.; Dekany, I.; Fendler, J. H. Ultrathin Graphite Oxide-Polyelectrolyte Composites Prepared by Self-Assembly: Transition between Conductive and Non-Conductive States. *Adv. Mater.* **1996**, *8*, 637–641.
30. Bonanni, A.; Chua, C. K.; Zhao, G. J.; Sofer, Z.; Pumera, M. Inherently Electroactive Graphene Oxide Nanoplatelets as Labels for Single Nucleotide Polymorphism Detection. *ACS Nano* **2012**, *6*, 8546–8551.
31. Ambrosi, A.; Chee, S. Y.; Khezri, B.; Webster, R. D.; Sofer, Z.; Pumera, M. Metallic Impurities in Graphenes Prepared from Graphite Can Dramatically Influence Their Properties. *Angew. Chem., Int. Ed.* **2012**, *51*, 500–503.
32. Ambrosi, A.; Chua, C. K.; Khezri, B.; Sofer, Z.; Webster, R. D.; Pumera, M. Chemically Reduced Graphene Contains Inherent Metallic Impurities Present in Parent Natural and Synthetic Graphite. *Proc. Natl. Acad. Sci. U.S.A.* **2012**, *109*, 12899–12904.
33. Paredes, J. I.; Villar-Rodil, S.; Martínez-Alonso, A.; Tascon, J. M. D. Graphene Oxide Dispersions in Organic Solvents. *Langmuir* **2008**, *24*, 10560–10564.
34. Rinaldi, A.; Frank, B.; Su, D. S.; Hamid, S. B. A.; Schlogl, R. Facile Removal of Amorphous Carbon from Carbon Nanotubes by Sonication. *Chem. Mater.* **2011**, *23*, 926–928.
35. Bonanni, A.; Ambrosi, A.; Pumera, M. On Oxygen-Containing Groups in Chemically Modified Graphenes. *Chem.—Eur. J.* **2012**, *18*, 4541–4548.
36. Liu, L. Q.; Qin, Y. J.; Guo, Z. X.; Zhu, D. B. Reduction of Solubilized Multi-Walled Carbon Nanotubes. *Carbon* **2003**, *41*, 331–335.
37. Kumar, P. V.; Bardhan, N. M.; Tongay, S.; Wu, J.; Belcher, A. M.; Grossman, J. C. Scalable Enhancement of Graphene Oxide Properties by Thermally Driven Phase Transformation. *Nat. Chem.* **2014**, *6*, 151–158.
38. Luo, J. Y.; Cote, L. J.; Tung, V. C.; Tan, A. T. L.; Goins, P. E.; Wu, J. S.; Huang, J. X. Graphene Oxide Nanocolloids. *J. Am. Chem. Soc.* **2010**, *132*, 17667–17669.
39. Eda, G.; Lin, Y. Y.; Mattevi, C.; Yamaguchi, H.; Chen, H. A.; Chen, I. S.; Chen, C. W.; Chhowalla, M. Blue Photoluminescence from Chemically Derived Graphene Oxide. *Adv. Mater.* **2010**, *22*, 505–509.
40. Cuong, T. V.; Pham, V. H.; Tran, Q. T.; Hahn, S. H.; Chung, J. S.; Shin, E. W.; Kim, E. J. Photoluminescence and Raman Studies of Graphene Thin Films Prepared by Reduction of Graphene Oxide. *Mater. Lett.* **2010**, *64*, 399–401.
41. Erickson, K.; Erni, R.; Lee, Z.; Alem, N.; Gannett, W.; Zettl, A. Determination of the Local Chemical Structure of Graphene Oxide and Reduced Graphene Oxide. *Adv. Mater.* **2010**, *22*, 4467–4472.
42. Zhang, B.; Fan, L.; Zhong, H.; Liu, Y.; Chen, S. Graphene Nanoelectrodes: Fabrication and Size-Dependent Electrochemistry. *J. Am. Chem. Soc.* **2013**, *135*, 10073–10080.
43. Xia, Z. Y.; Pezzini, S.; Treossi, E.; Giambastiani, G.; Corticelli, F.; Morandi, V.; Zanelli, A.; Bellani, V.; Palermo, V. The Exfoliation of Graphene in Liquids by Electrochemical, Chemical, and Sonication-Assisted Techniques: A Nano-scale Study. *Adv. Funct. Mater.* **2013**, *23*, 4684–4693.
44. Si, Y.; Samulski, E. T. Synthesis of Water Soluble Graphene. *Nano Lett.* **2008**, *8*, 1679–1682.
45. Pan, S. Y.; Aksay, I. A. Factors Controlling the Size of Graphene Oxide Sheets Produced via the Graphite Oxide Route. *ACS Nano* **2011**, *5*, 4073–4083.
46. Dresselhaus, M. S.; Jorio, A.; Hofmann, M.; Dresselhaus, G.; Saito, R. Perspectives on Carbon Nanotubes and Graphene Raman Spectroscopy. *Nano Lett.* **2010**, *10*, 751–758.
47. Englert, J. M.; Dotzer, C.; Yang, G. A.; Schmid, M.; Papp, C.; Gottfried, J. M.; Steinruck, H. P.; Specker, E.; Hauke, F.; Hirsch, A. Covalent Bulk Functionalization of Graphene. *Nat. Chem.* **2011**, *3*, 279–286.
48. Hummers, W. S.; Offeman, R. E. Preparation of Graphitic Oxide. *J. Am. Chem. Soc.* **1958**, *80*, 1339–1339.
49. Cote, L. J.; Kim, F.; Huang, J. X. Langmuir-Blodgett Assembly of Graphite Oxide Single Layers. *J. Am. Chem. Soc.* **2009**, *131*, 1043–1049.